Computers in Biology and Medicine xxx (xxxx) 110189

Contents lists available at ScienceDirect

Computers in Biology and Medicine

journal homepage: www.elsevier.com/locate/compbiomed

The geometric relationship between root length and root surface area determined from digital tooth models

Chloe Xiao Wei Chan [a], Wee Kheng Leow [b], Alan Ho-lun Cheng [b], Kelvin Weng Chiong Foong [c], *

[a] Discipline of Orthodontics Faculty of Dentistry, National University of Singapore, Singapore
[b] Department of Computer Science, School of Computing, National University of Singapore, Singapore
[c] Orthodontics Residency Training Programme Faculty of Dentistry, National University of Singapore, Singapore

ARTICLE INFO

Keywords:
Root length
Root surface area
Root cross-sectional area
Python algorithm
3D tooth models
External apical root resorption

ABSTRACT

Aim: This study investigated the correlation between root length (RL) and root surface area (RSA) in permanent maxillary and mandibular teeth to understand the impact of external apical root resorption.

Materials and methods: Three-dimensional (3D) models of human teeth, representing a Japanese male adult population, were sourced from a commercial provider and segmented into individual roots. A Python algorithm calculated root surface area (RSA) at simulated root lengths by virtually shortening the roots in 1 mm increments. The total RSA (tRSA) was determined by combining the circumferential root surface area (cRSA) with the cross-sectional area (CSA).

Results: Maxillary and mandibular first molars exhibited the largest tRSAs in their respective arches. In the initial 3 mm of simulated root shortening, five of seven maxillary and mandibular tooth types exhibited minimal tRSA reduction, averaging less than 7 %. Beyond 3 mm, tRSA reduction became more pronounced, an average of 19.4 % for maxillary teeth and 27.77 % for mandibular teeth. CSA significantly contributes to tRSA; the average CSA proportion increases progressively with greater root length reduction, particularly when it exceeds 8 mm.

Conclusion: RSA together with CSA, not just root length, is a crucial consideration when assessing the clinical impact from root length reduction. Generally, when root length loss is up to 20 % (~3 mm), more than 90 % of the tRSA remains. Teeth with higher CSA proportions, such as molars, are better equipped to retain periodontal support despite substantial RL loss, owing to their broader girth.

1. Introduction

The permanent human dentition consists of 32 teeth: 16 in the maxillary arch (upper jaw) and 16 in the mandibular arch (lower jaw). Each tooth comprises a crown, visible above the gum line, and one or more roots embedded in the jawbone which anchor the crown and provide stability for chewing and aesthetics. This stability relies on three key factors: root length (RL), root surface area (RSA), and the amount of bone covering the root surface. Two pathological conditions can compromise this stability: (i) external apical root resorption (EARR) [1], where root length decreases from the tip toward the crown, and (ii) periodontal bone loss, where bone levels recede from the crown toward the root tip, exposing the roots above the gum margin. Both conditions reduce the RSA, leading to compromised tooth stability. Severe RSA loss increases tooth mobility, diminishing the tooth's ability to support chewing forces [2]. Additionally, teeth with significantly reduced RSA may drift from their normal positions, adversely affecting dental aesthetics and function [3].

Understanding the relationship between RL and RSA is essential for predicting the impact of root length loss on tooth stability. RSA represents the periodontal attachment area, where the tooth root is connected to the surrounding alveolar bone via the periodontal ligament, a critical structure for tooth stability and function. Human tooth roots have a conical shape, narrowing from the broader base at the cementoenamel junction (CEJ) to the apex. The CEJ, a sinuous circumscribing line where the root merges with the crown, marks this transition. Studies on single-rooted teeth in European adults [4,5] confirmed the conical nature of these teeth by analysing root taper. This taper implies that a given amount of EARR results in a smaller loss of periodontal attach-

* Corresponding author. Orthodontics Residency Training Programme Faculty of Dentistry, National University of Singapore, 9 Lower Kent Ridge Road, #10-01, Singapore, 119085, Singapore.

E-mail addresses: chloec@u.nus.edu (C.X. Wei Chan), leowwk@comp.nus.edu.sg (W.K. Leow), hcheng@comp.nus.edu.sg (A.H.-l. Cheng), denfwc@nus.edu.sg (K.W. Chiong Foong).

https://doi.org/10.1016/j.compbiomed.2025.110189
Received 17 June 2024; Received in revised form 21 March 2025; Accepted 8 April 2025
0010-4825/© 20XX

ment area compared to an equivalent amount of crestal bone loss from the gum margin due to periodontitis.

Several studies have investigated RSA to understand the effects of periodontal attachment loss on root surface area. Division planimetry was used with a calibrated opisometer to measure root contours and RSA [6]. Another study employed a membrane technique combined with image analysis software to quantify RSA at various simulated attachment levels [7]. Computer image analysis was used to measure RSA for mandibular canines and premolars, reporting mean RSA values of 275.88 mm^2 for mandibular canines, 251.45 mm^2 for first premolars, and 271.81 mm^2 for second premolars [8]. More recently, micro-computed tomography (micro-CT) scans were used to create 3D tooth models for evaluating RSA [9].

Focusing on apical length loss, a study [10] mathematically calculated the periodontal attachment area on a single maxillary central incisor through stepwise 1 mm reductions of root length from the apex. It found that 3 mm of apical resorption resulted in a similar remaining attachment area as 1 mm of crestal bone loss, and concluded that apical resorption caused less periodontal attachment loss compared to crestal attachment loss within the first 3 mm of root loss. Beyond 3 mm, the ratio became less favorable, with 2 mm of apical root loss equating to 1 mm of crestal bone loss. The relationship between RL and RSA was further explored by directly measuring RSA using Cone Beam Computed Tomography (CBCT) scans with a dedicated algorithm [11]. It observed that RSA is not determined solely by RL but also by factors such as the number of roots, root curvature, and the presence of furcations. These two studies collectively highlight the complexity of the relationship between RL and RSA, emphasizing the importance of appropriate methodologies to better assess the morphological nature of root length loss on tooth stability.

When EARR is detected, clinicians are primarily concerned with the long-term prognosis of the affected tooth. While studies indicate that even severely resorbed roots may have minimal impact on the tooth's longevity and functionality [2,3], clinicians still need to assess the extent of resorption and potential risks. A critical factor in determining the prognosis is the remaining RSA and its associated periodontal attachment area. Clinicians need to evaluate if enough periodontal attachment to the surrounding alveolar bone remains to provide sufficient support for the tooth's long-term stability. Moving teeth with substantial EARR by orthodontic appliances will also require special biomechanical consideration since the tooth's center of resistance changed with a reduction in root length.

The most direct approach to quantifying EARR, using periapical radiographs, involves the subtraction of the measured post-treatment tooth length from the pre-treatment tooth length [12]. To overcome the possibility of radiographic image distortion with periapical radiographs, the rule-of-three formula [13] calculated the ratio between the initial and final root length, using the ratio between the initial and final crown length as the magnification factor.

Previous methods for assessing root resorption and RSA have notable limitations and gaps. First, direct radiographic measurements of root length, while informative, fail to capture the three-dimensional complexity of root morphology and its influence on periodontal attachment. Measuring RSA provides a more comprehensive understanding of the effects of apical root shortening, but earlier methods did not consider the CSA of the root at different levels of root shortening. This omission emphasises the need for more accurate techniques that account for the three-dimensional nature of root morphology and the effects of root length loss on periodontal attachment. No known studies have measured the CSA at simulated root shortening or integrated CSA and circumferential root surface area (cRSA) to represent total RSA (tRSA) as a proxy for periodontal attachment area. Furthermore, 3D studies of RSA require specialised equipment, software, and expertise for image acquisition, processing, and analysis, making these resource-intensive methods less accessible and limiting their widespread adoption in studying the impact of root length reduction on RSA.

This study intends to establish baseline information on the geometric relationship between RL and RSA in permanent teeth using 3D human tooth models. It will include CSA into RSA calculations to enhance the methodology, offering a more accurate and comprehensive representation of the periodontal attachment surface area following simulated external apical resorption. Addressing the limitations of previous approaches, this study seeks to enhance understanding of how root length reduction impacts RSA to offer valuable insights into the anatomical changes associated with EARR.

To achieve this, the study will develop an algorithm using *Python*, a free, versatile, and beginner-friendly programming language, to calculate both cRSA and CSA at various levels of simulated root length reduction. This approach will allow for a detailed analysis of how CSA contributes to tRSA across varying degrees of root length reduction, from minimal to severe.

The findings will provide critical baseline data on the relationship between root length and RSA, which is a key determinant of tooth stability. RSA, when incorporating CSA, serves as a more accurate measure of the remaining tooth support and a better predictor of tooth stability. A greater understanding of this relationship can guide clinicians in treatment planning and decision-making for managing root resorption cases. The study ultimately addresses the central question: What is the correlation between root length and RSA in permanent maxillary and mandibular teeth? By answering this, it aims to lay the groundwork for future research and clinical applications in dentistry.

2. Material and methods

2.1. 3D model acquisition

The 3D models of human permanent teeth used in this study were obtained as STL files from a commercial source: https://www.cgtrader.com/3d-print-models/science/biology/dental-anatomy-model-with-natural-root-anatomy-with-pulp. According to the vendor, these models were based on the dentition of Japanese male adults aged 20–30 years. They were selected for this study due to their anatomical accuracy in representing the root shape, root length, and crown morphology of permanent incisors, canines, premolars, and first and second molars, as illustrated in Fig. 1. High-resolution mesh data for six of the 14 tooth types are shown in Fig. 2.

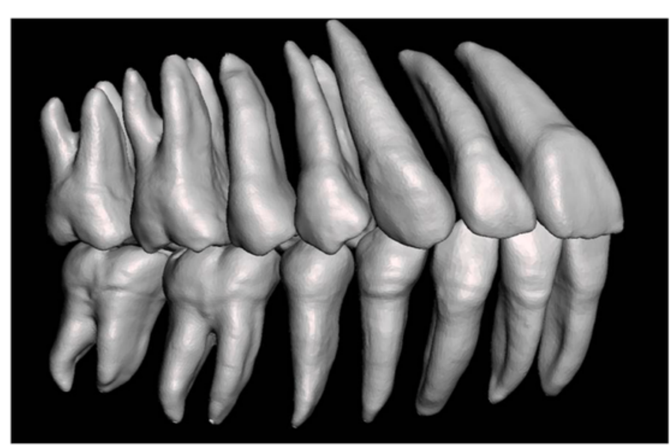

Fig. 1. Discrete surface mesh models of maxillary and mandibular right central incisors to second molars, 14 teeth in total.

Tooth	STL	Triangles	Vertices
#11		17,106	51,318
#13		11,325	33,975
#16		57,806	173,418

Tooth	STL	Triangles	Vertices
#41		11,164	33,492
#43		15,020	45,060
#46		34,472	103,416

Fig. 2. Mesh data of maxillary (left) and mandibular (right) teeth models [Microsoft 3D Viewer version 7.2407.16012.0 (2017)].

2.2. Why sample size calculation was not performed

A sample size calculation was not performed for this study because statistical power analysis is not required for studies that are not hypothesis driven. This study aimed to characterise the geometric relationship between RL and RSA using anatomically realistic 3D tooth models. It did not involve testing differences between groups or making inferences about a larger population. The primary intent was to establish baseline information on the geometric relationship between RL and RSA in permanent teeth that could be used as a foundational reference for future research and clinical applications.

2.3. Segmentation of tooth root from crown

Utilising Meshmixer Version 3.3 (Autodesk, 2022), the roots of each three-dimensional tooth model were separated from the crowns at the presumptive cemento-enamel junction (CEJ) through a semi-automated process by an experienced clinician. The CEJ on the 3D tooth model is a curvi-linear circumscribe line that demarcates the crown from the root. The process for segmenting the maxillary right central incisor is shown in Fig. 3 (a & b). Root length (RL) measurement was determined from the root apex to the CEJ's highest inflection point (Fig. 3c).

The root portions of each multi-rooted tooth were segmented into individual roots, resulting in two distinct roots for teeth #46 and #47 (the mandibular right first and second molars, respectively) and three distinct roots for teeth #16 and #17 (the maxillary right first and second molars) as shown in Fig. 4. Each root was saved as a separate.PLY file to enable precise measurements, as illustrated in Fig. 5.

The process of segmenting the maxillary right first molar #46 and one of the three roots (mesio-buccal root) is shown in Fig. 5.

2.4. Determining the root length and root surface area

To calculate the root surface area (RSA) (mm^2) based on a given root length (RL) (mm), an algorithm was implemented in Python (Version 3.9, Python Software Foundation, 2022) along with NumPy and PyVista packages.

A three-dimensional (3D) model of the tooth is represented by a triangular mesh that contains n mesh points $\mathbf{x}_i$ for $i = 1, \cdots, n$. Principal component analysis (PCA) [20] is applied as follows to identify the three principal directions of the tooth model:

1. Compute the mean $\boldsymbol{\mu}$ of mesh points:

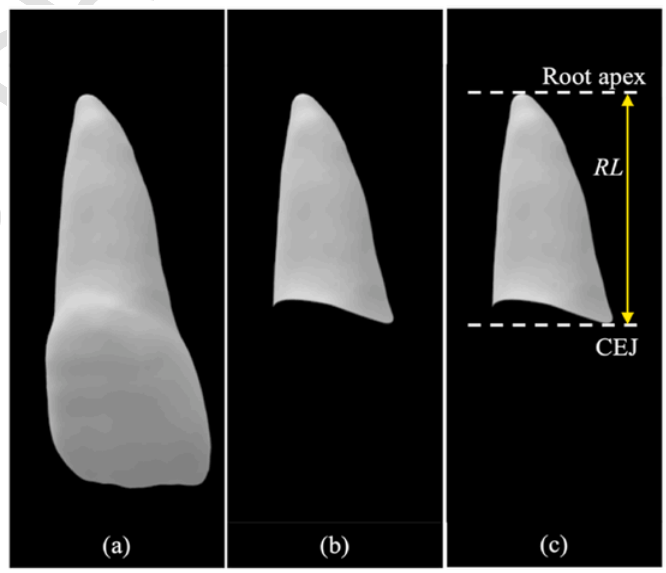

Fig. 3. (a) 3D tooth model of the upper right central incisor. (b) 3D root model after separation from the crown at the CEJ. (c) Root length (*RL*) measurement from highest inflection point along the CEJ to the root apex.

$$\boldsymbol{\mu} = \frac{1}{n}\sum_{1}^{n}\mathbf{x}_i.$$

2. Compute covariance matrix $\mathbf{C}$:

$$\mathbf{C} = \frac{1}{n}\sum_{1}^{n}\left(\mathbf{x}_i - \boldsymbol{\mu}\right)\left(\mathbf{x}_i - \boldsymbol{\mu}\right)^{\mathrm{T}}.$$

3. Apply eigendecomposition to covariance matrix $\mathbf{C}$:

$$\mathbf{C} = \mathbf{Q}\boldsymbol{\Lambda}\mathbf{Q}^{\mathrm{T}},$$

Where $\mathbf{Q}$ contains the eigenvectors in its columns and $\boldsymbol{\Lambda}$ is a diagonal matrix of the corresponding eigenvalues of the eigenvectors. In NumPy, eigendecomposition can be performed using the numpy.linalg.eig function.

The first principal direction $\mathbf{v}_1$ is the eigenvector in $\mathbf{Q}$ with the largest eigenvalue. It corresponds to the long axis of the tooth. The

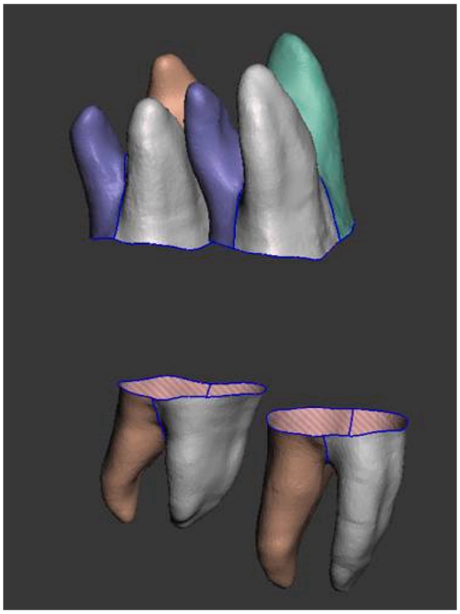

Fig. 4. Segmentation of multi-rooted teeth #16, #17 (top row) and #46, #47 (bottom row).

points along the long axis that correspond to the apex and CEJ are determined, and the distance between these points gives the root length.

Let $\mathbf{p}_j$ denote the j-th landmark point, for $j = 0, \ldots, m$, along the long axis $\mathbf{v}_1$ starting from the apex point stepwise in increments of 1 mm. It can be obtained as follows:

$$\mathbf{p}_j = \mathbf{p}_0 + j\mathbf{v}_1,$$

where $\mathbf{p}_0$ denotes the position of the root apex at 0 mm along $\mathbf{v}_1$, and m denotes the number of landmark points along the long axis. A plane is placed at landmark point $\mathbf{p}_j$ such that its surface normal is parallel to the long axis $\mathbf{v}_1$. This plane sections the tooth model at point $\mathbf{p}_j$. Sectioning of a mesh model by a plane can be performed by the PyVista function pyvista.DataSetFilters.clip, where pyvista.DataSetFilters refers to the tooth model. The tooth surface area a_j above the plane is determined by the PyVista function pyvista.DataSet.area. This calculation is repeated for each landmark point $\mathbf{p}_j$, starting at 1 mm from the root apex, to obtain the tooth surface area a_j that corresponds to a specific root length l_j. Since the landmark points are spaced out at 1 mm interval along the long axis $\mathbf{v}_1$, the length l_j is equal to j mm.

The algorithm for measuring root surface can be summarised as follows.

2.4.1. Root surface measurement

1. Apply pyvista.read to read a tooth model, call it root, from mesh file. The list of mesh points are kept in root.points.
2. Form the covariance matrix $\mathbf{C}$ from the mesh points root.points.
3. Apply numpy.linalg.eig to $\mathbf{C}$ to obtain the eigenvector matrix $\mathbf{Q}$ and eigenvalue matrix $\mathbf{\Lambda}$.
4. Identify the eigenvector $\mathbf{v}_1$ in $\mathbf{Q}$ with the largest eigenvalue.
5. For $j = 1, \ldots, m$,
6. Obtain landmark point $\mathbf{p}_j$ located at j mm from the root apex $\mathbf{p}_0$ along the long axis $\mathbf{v}_1$.
7. Apply pyvista.Plane to form a plane located at landmark point $\mathbf{p}_j$ whose surface normal is $\mathbf{v}_1$.
8. Apply pyvista.DataSetFilters.clip to clip the tooth model root with the plane.
9. Obtain surface area of the clipped tooth model from root.area.
10. Save root length $l_j = j$ and root surface area.

For a tooth with multiple roots, the distance from the most mesial to the most distal points of the CEJ may be larger than the distance from the apex to the CEJ. Consequently, the direction from the root apex to the CEJ would be given by the second or third principal direction, instead of the first principal direction. In this case, the appropriate principal direction is selected manually, and the same algorithm is applied along the selected direction to calculate root lengths and root surface areas.

The surface area of the roots, including the cross-sectional area, was calculated by defining horizontal slices along the root's long axis in

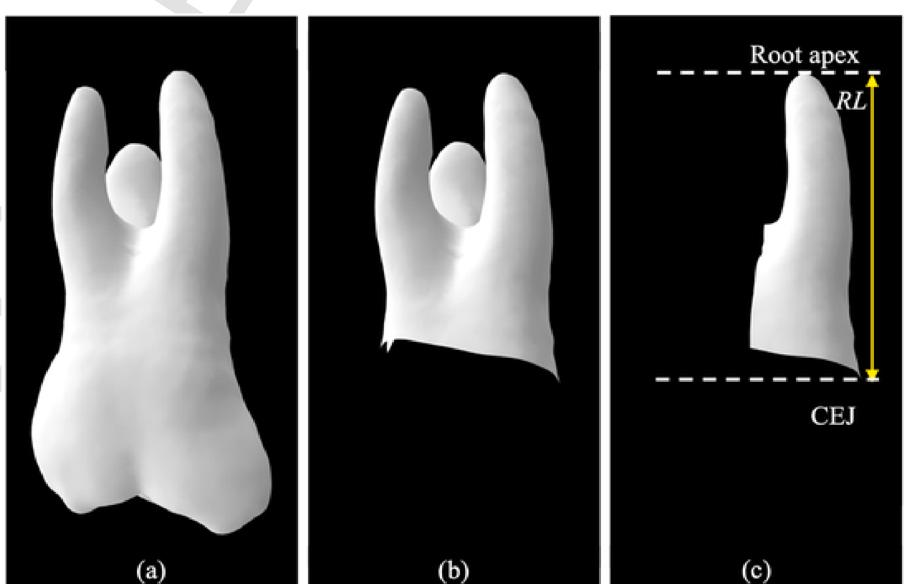

Fig. 5. (a) 3D tooth model of the maxillary right first molar. (b) 3D root model after separation from the crown at the CEJ. (c) Root length (*RL*) measurement from highest inflection point along the CEJ to the root apex of the mesio-buccal root (one of three roots).

1 mm increments from the apex. The corresponding RSA, highlighted as 1 mm thick colored bands for each root length from the CEJ to the apex, is shown for #11 and #16 in Figs. 6 and 7, respectively. The 1 mm root length increments for RSA calculations were adapted from a previous study [10], which simulated 1 mm root shortening to calculate remnant periodontal attachment areas for a permanent upper incisor. The internal anatomy of each root in the 3D models, including the root canal, is depicted in Fig. 8. Cross-sectional area calculations account for the root canal space to ensure a more accurate representation of the periodontal attachment area at each cross-section.

Root measurements will be analysed and tabulated using the following nomenclature.

- **RL**: Root length.

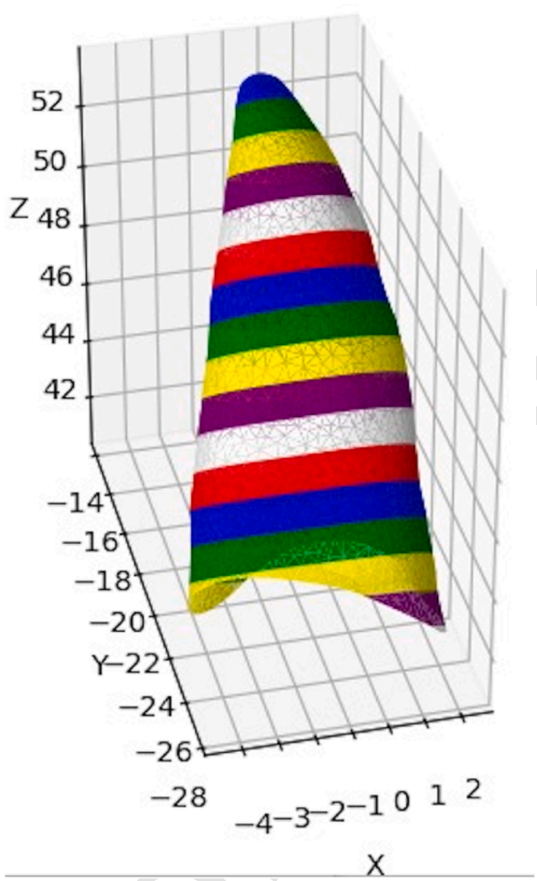

Fig. 6. Measurement of #11 root length and root surface area in 1 mm increments from the root apex.

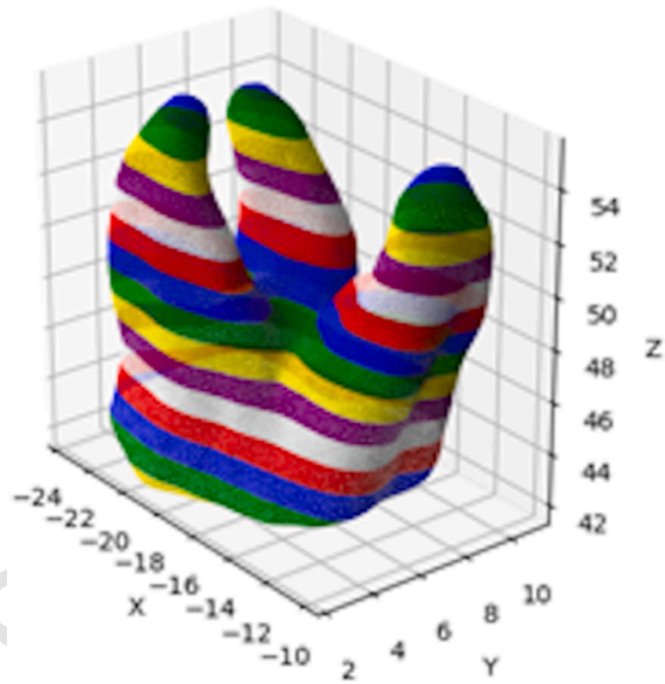

Fig. 7. Measurement of #16 root length and root surface area in 1 mm increments from the root apex.

- **cRSA**: Circumferential root surface area, excluding the root cross-sectional area at the simulated root length loss, calculated from the CEJ to the simulated root length.
- **CSA**: Cross-sectional area of the root created perpendicular to the tooth's long axis.
- **tRSA**: Total root surface area, calculated as the sum of cRSA and CSA.

3. Results

3.1. Root length (RL) and total root surface area (tRSA) observations

Root length (RL) and total root surface area (tRSA) data for teeth #11–17 and #41–47 are summarised in Tables 1 and 2. Among maxillary single-rooted teeth (#11, #12, #13, and #15), the largest tRSA is 265.42 mm^2 for tooth #13, while the smallest is 206.19 mm^2 for tooth #12. For mandibular single-rooted teeth (#41, #42, #43, #44, and #45), the largest tRSA is 218.80 mm^2 for tooth #43, and the smallest is 143.80 mm^2 for tooth #41. Teeth #13 and #43 also have the longest roots, measuring 19 mm and 16 mm, respectively. Maxillary first molars (#16), with three roots, and mandibular first molars (#46), with two roots, exhibit the largest tRSA values at 444.17 mm^2 and

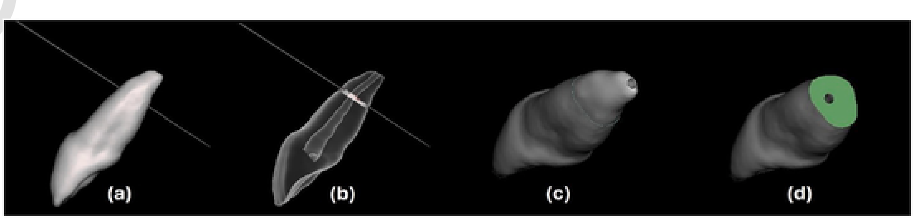

Fig. 8. Creating the cross-sectional area with the following steps: (a) a simulated plane cut near the root apex of the STL tooth model, perpendicular to the tooth's long axis; (b) a transparent 3D tooth model revealing the internal root canal structure; (c) the circumscribed line at the root surface from the plane cut; and (d) the cross-sectional surface, highlighting the root canal space at its center.

Table 1
Maxillary root length measurements and corresponding total root surface areas (prior to simulated root length reduction).

Maxillary	#11	#12	#13	#14	#15	#16	#17
RL (mm)	17	16	19	17	15	14[a]	13[a]
tRSA (mm^2)	239.47	206.19	265.42	291.90	239.01	444.17	328.67

[a] The value recorded is the length of the longest discrete root of each multi-rooted tooth following segmentation.

Table 2
Mandibular root length measurements and corresponding total root surface areas (prior to simulated root length reduction).

Mandibular	#41	#42	#43	#44	#45	#46	#47
RL (mm)	12	13	16	14	14	15[a]	14[a]
tRSA (mm^2)	143.80	158.49	218.80	197.90	194.17	351.01	260.67

[a] The value recorded is the length of the longest discrete root of each multi-rooted tooth following segmentation.

351.01 mm^2, respectively. Among multi-rooted teeth, the smallest tRSA values are observed in #14 (maxillary segment, 291.90 mm^2) and #47 (mandibular segment, 260.67 mm^2).

3.2. Root lengths and corresponding root surface area data

Root lengths and root surface area data are summarised in Tables 3–8 for six teeth: maxillary and mandibular central incisors (#11, #41), canines (#13, #43), and first molars (#16, #46). RL and RSA data for the entire set of 14 teeth are available in the Annex.

3.3. Guide to reading Tables 3–8

- **Column A:** Simulated apical root shortening from full root length (RL).
- **Column B:** Percentage reduction of RL.
- **Column C:** Circumferential root surface area (cRSA), excluding the cross-sectional area at the RL reduction level.
- **Column D:** Cross-sectional area (CSA) at the RL reduction level.
- **Column E:** Total root surface area (tRSA), calculated as cRSA + CSA.
- **Columns F and G:** Remaining percentage of tRSA and percentage reduction in tRSA, respectively.

Table 3
Root length and root surface area of #11 – the maxillary right central incisor.

A	B	C	D	E	F	G
Root length	Reduction of RL	cRSA	CSA	tRSA	Remnant tRSA	Reduction of tRSA
(mm)	(%)	(mm^2)	(mm^2)	(mm^2)	(%)	(%)
17	–	239.47	–	239.47	100.00	–
16	5.88	239.16	0.16	239.32	99.94	0.06
15	11.77	234.68	1.37	236.05	98.57	1.43
14	17.65	223.54	27.14	250.68	104.68	−4.68
13	23.53	204.67	34.19	238.86	99.75	0.25
12	29.41	183.56	32.05	215.61	90.04	9.96
11	35.29	162.96	30.89	193.85	80.95	19.05
10	41.18	142.66	29.7	172.36	71.98	28.02
9	47.06	122.82	28.15	150.97	63.04	36.96
8	52.94	103.61	25.58	129.19	53.95	46.05
7	58.83	85.48	22.46	107.94	45.07	54.93
6	64.71	68.61	19.5	88.11	36.79	63.21
5	70.59	52.94	16.45	69.39	28.98	71.02
4	76.48	38.56	12.88	51.44	21.48	78.52
3	82.35	26.01	9.38	35.39	14.78	85.22
2	88.24	15.40	6.05	21.45	8.96	91.04
1	94.12	6.92	3.79	10.71	4.47	95.53

Table 4
Root length and root surface area of #13 – the maxillary right canine.

A	B	C	D	E	F	G
Root length	Reduction of RL	cRSA	CSA	tRSA	Remnant tRSA	Reduction of tRSA
(mm)	(%)	(mm^2)	(mm^2)	(mm^2)	(%)	(%)
19	–	265.42	–	265.42	100	–
18	5.26	265.10	0.05	265.15	99.90	0.10
17	10.53	261.74	0.28	262.02	98.72	1.28
16	15.79	255.61	4.91	260.52	98.15	1.85
15	21.05	239.85	30.34	270.19	101.80	−1.80
14	26.32	218.17	33.85	252.02	94.95	5.05
13	31.58	196.53	32.31	228.84	86.22	13.78
12	36.84	175.14	30.11	205.25	77.33	22.67
11	42.11	154.24	27.55	181.79	68.49	31.51
10	47.37	134.06	25.16	159.22	59.99	40.01
9	52.63	114.72	22.93	137.65	51.86	48.14
8	57.89	96.35	20.42	116.77	43.99	56.01
7	63.16	79.18	18.29	97.47	36.72	63.28
6	68.42	63.14	16.07	79.21	29.84	70.16
5	73.68	48.40	13.6	62.00	23.36	76.64
4	78.95	35.05	11.12	46.17	17.39	82.61
3	84.21	23.22	8.24	31.46	11.85	88.15
2	89.47	13.36	5.3	18.66	7.03	92.97
1	94.74	5.63	2.94	8.57	3.23	96.77

Table 5
Root length and root surface area of #16 – the maxillary right first molar.

A	B	C	D	E	F	G
Root length	Reduction of RL	cRSA	CSA	tRSA	Remnant tRSA	Reduction of tRSA
(mm)	(%)	(mm^2)	(mm^2)	(mm^2)	(%)	(%)
14	–	444.17	–	444.17	100	–
13	7.14	440.61	3.3	443.91	99.94	0.06
12	14.29	413.69	29.58	443.27	99.80	0.20
11	21.43	380.78	73.33	454.11	102.24	−2.24
10	28.57	347.67	106.44	454.11	102.24	−2.24
9	35.71	313.38	77.64	391.02	88.03	11.97
8	42.86	275.31	78.79	354.10	79.72	20.28
7	50.00	223.17	79.26	302.43	68.09	31.91
6	57.14	173.45	63.2	236.65	53.28	46.72
5	64.29	129.87	106.78	236.65	41.22	58.78
4	71.43	90.53	44.97	135.50	30.77	69.23
3	78.57	56.17	80.48	136.65	30.51	69.49
2	85.71	27.17	28.97	56.14	12.64	87.36
1	92.86	8.93	12.92	21.85	4.92	95.08

Table 6
Root length and root surface area of #41 – the mandibular right central incisor.

A	B	C	D	E	F	G
Root length	Reduction of RL	cRSA	CSA	tRSA	Remnant tRSA	Reduction of tRSA
(mm)	(%)	(mm^2)	(mm^2)	(mm^2)	(%)	(%)
12	–	143.80	–	143.80	100	–
11	8.33	136.64	10.37	147.01	102.23	−2.23
10	16.67	122.39	14.08	136.47	94.90	5.10
9	25.00	107.85	13.92	121.77	84.68	15.32
8	33.33	93.18	13.4	106.58	74.12	25.88
7	16.67	78.60	12.49	91.09	63.35	36.65
6	50.00	64.31	11.55	75.86	52.75	47.25
5	58.33	50.59	10.73	61.32	42.64	57.36
4	66.67	37.46	9.92	47.38	32.95	67.05
3	75.00	25.24	8.27	33.51	23.30	76.70
2	83.33	14.43	6.31	20.74	14.43	85.57
1	91.67	5.52	3.18	8.70	6.05	93.95

Table 7
Root length and root surface area of #43 – the mandibular right canine.

A	B	C	D	E	F	G
Root length	Reduction of RL	cRSA	CSA	tRSA	Remnant tRSA	Reduction of tRSA
(mm)	(%)	(mm^2)	(mm^2)	(mm^2)	(%)	(%)
16	–	218.80	–	218.80	100	–
15	6.25	218.13	0.61	218.74	99.98	0.02
14	12.5	210.62	4.84	215.46	98.48	1.52
13	18.75	199.75	9.05	208.80	95.43	4.57
12	25	186.78	12.24	199.02	90.96	9.04
11	31.25	172.30	14.76	187.06	85.50	14.50
10	37.5	156.35	17.17	173.52	79.31	20.69
9	43.75	139.02	19.55	158.57	72.47	27.53
8	50	120.44	22.16	142.60	65.18	34.82
7	56.25	100.94	25.62	126.56	57.84	42.16
6	62.50	80.97	26.77	107.74	49.24	50.76
5	68.75	60.92	26.33	87.25	39.88	60.12
4	75.00	40.93	26.86	67.79	30.98	69.02
3	81.25	21.14	25.37	46.51	21.26	78.74
2	87.5	8.26	6.51	14.77	6.75	93.25
1	93.75	2.79	0.11	2.90	1.33	98.67

Table 8
Root length and root surface area of #46 – the mandibular right first molar.

A	B	C	D	E	F	G
Root length	Reduction of RL	cRSA	CSA	tRSA	Remnant tRSA	Reduction of tRSA
(mm)	(%)	(mm^2)	(mm^2)	(mm^2)	(%)	(%)
15	–	351.01	–	351.01	100	–
14	6.67	350.91	0.1	351.01	100.00	0.00
13	13.33	343.23	4.6	347.83	99.10	0.90
12	20.00	328.39	11.43	339.82	96.81	3.19
11	26.67	307.01	18.04	325.05	92.60	7.40
10	33.33	281.62	23.72	305.34	86.99	13.01
9	40.00	252.83	39.77	292.60	83.36	16.64
8	46.67	221.25	33.69	254.94	72.63	27.37
7	53.33	186.77	50.3	237.07	67.54	32.46
6	60	149.64	53.43	203.07	57.86	42.14
5	66.67	109.66	51.13	160.79	45.81	54.19
4	73.33	71.56	59.78	131.34	37.42	62.58
3	80	42.14	29.67	71.81	20.46	79.54
2	86.67	22.20	16.68	38.88	11.08	88.92
1	93.33	8.04	6.34	14.38	4.10	95.90

3.4. General observations of root length and the corresponding cRSA and tRSA

Across all 14 tooth types, cRSA decreases linearly with root length reduction (Tables 3–8). In contrast, tRSA shows minor fluctuations within the first 3–4 mm of root length reduction, influenced by the inclusion of CSA (Tables 3–6). The steepest reduction rates occur with greater root reductions, typically exceeding 50 %. While tRSA occasionally fluctuates due to CSA changes, these do not significantly affect the overall trends. Molar teeth exhibit substantially higher cRSA and tRSA values compared to incisors and canines. When root length loss is up to 20 % (~3 mm), more than 90 % of the tRSA remains.

The geometric relationship between root length and root surface area for the 14 tooth types is illustrated in two figures: Fig. 9 shows single-rooted tooth types, while Fig. 10 depicts multi-rooted first and second molars. These figures reveal two patterns in the net and percentage of remaining total root surface area (tRSA) after simulated root resorption. Firstly, for maxillary and mandibular teeth, the plotted lines exhibit a gradual slope for the first 1–3 mm, followed by a steeper decline beyond 3 mm of root length reduction. Secondly, the gradient becomes steeper only after 4–5 mm of root length reduction in maxillary and mandibular first and second molars, in contrast to incisors, canines, and premolars, where the steeper gradient begins earlier after 2–4 mm of root length reduction.

Table 9 records the average percentage reduction in tRSA for every 1 mm of root length reduction for the first 1–3 mm, for the subsequent 5 mm, and beyond 8 mm for all tooth types.

3.5. Simulated shortening of the first 3 mm of root length

In the maxillary arch, the average percentage reduction of RSA was less than 5 % - lateral incisor (3.03 %), canine (1.08 %), first (1.74 %) and second (3.15 %) premolars and the second molar (1.32 %). In contrast, the central incisor and the first molar gained tRSA by 1.06 % and 0.66 %, respectively. On average, the seven maxillary tooth types showed an average tRSA reduction of 1.22 %.

Compared with the maxillary teeth, the average reduction of RSA was more pronounced among five mandibular teeth – central incisor (6.06 %), lateral incisor (3.98 %), canine (2.04 %), first premolar (3.51 %) and first molar (1.36 %). Marginal average gains in tRSA were noted for the second premolar (1.53 %) and the second molar (0.5 %). On average, the seven mandibular tooth types showed an average tRSA reduction of 2.13 %.

3.6. Simulated shortening of the next 5 mm of root length (4th to 8th mm)

Beyond the initial 3 mm of root length reduction, the percentage reduction in tRSA becomes substantially more pronounced for each tooth type for the next 5 mm of simulated apical root shortening. In the maxillary arch, the reduction of tRSA ranged from a minimum of 14.24 % for the maxillary canine to the maximum of 22.90 % for the maxillary second premolar. The average reduction in tRSA for maxillary tooth types is 19.4 %. The mandibular central incisor showed the highest average percentage of tRSA reduction at 46.84 %. The lowest average percentage reduction in tRSA for mandibular teeth roots was with the second molar at 15.54 %. An average tRSA reduction of 27.77 % was calculated for all mandibular tooth types over the next 5 mm of root length reduction.

3.7. Simulated shortening beyond 8 mm of root length

All seven maxillary tooth types show a greater average loss of tRSA when RL loss extends beyond 8 mm compared with the average rate of loss in the initial first 3 mm and between 4 and 8 mm of RL reduction. Out of the seven mandibular tooth types, the average tRSA reduction of #43, #44, #46 and #47 exceeded the average within the first 3 mm and the next 5 mm of RL reduction.

The principal observations on the reduction of tRSA, derived from the three levels of RL reduction, are summarised in Tables 10 and 11.

3.8. Significant contribution of CSA to tRSA

At each 1 mm of RL reduction, the CSA combines with the circumferential root surface area (cRSA) to form the total root surface area (tRSA). Although CSA is generally smaller than cRSA, as shown in Tables 3–8, it significantly contributes to tRSA. The average CSA proportion increases progressively with greater RL reduction, particularly when RL reduction exceeds 8 mm, as illustrated in Fig. 11.

The tooth-specific trends reveal distinct variations in the contribution of CSA to tRSA during RL reduction. For the maxillary central incisor (#11), the CSA proportion is at a moderate 3.8 % within the 1–3 mm RL reduction range and increases steadily to 25.2 % when the RL reduction exceeds 8 mm. In contrast, the maxillary canine (#13) exhibits a consistently lower CSA contribution, starting at just 0.7 % within the 1–3 mm RL reduction range and rising to 22.4 % for reductions exceeding 8 mm. The maxillary first molar (#16) shows the most significant increase, with CSA accounting for 7.9 % with the 1–3 mm

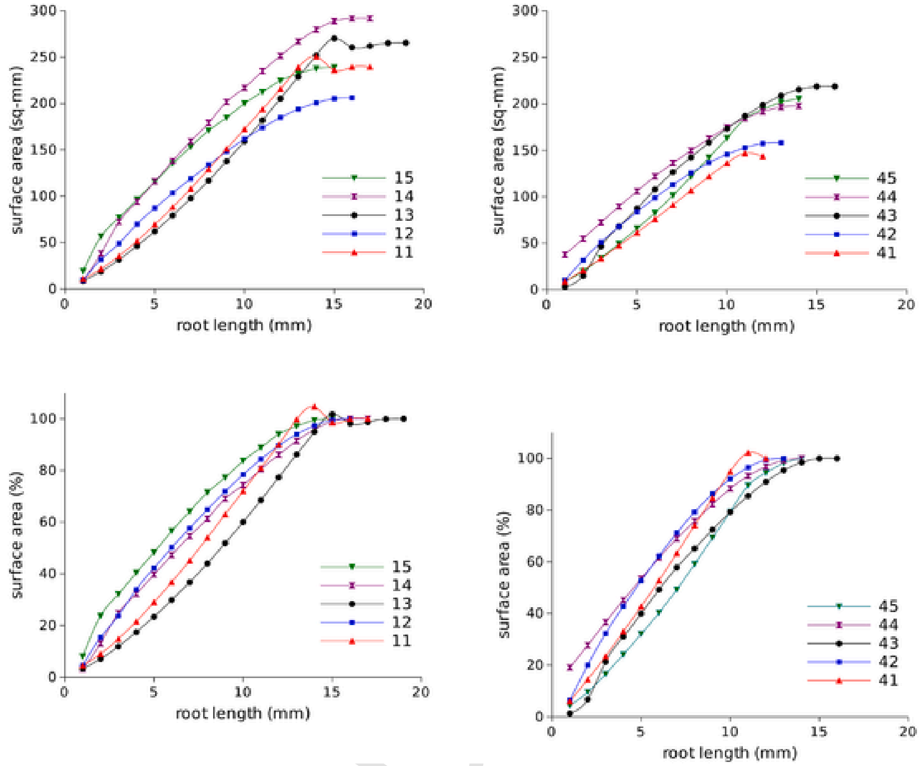

Fig. 9. Relationship of RL and tRSA of 5 tooth types - from maxillary and mandibular central incisors to second premolars. The top row of two graphs shows the net remnant tRSA of the maxillary (left graph) and mandibular (right graph) incisors, canines, and premolars. The bottom row of two graphs represents the percentage of remnant tRSA for the same tooth types.

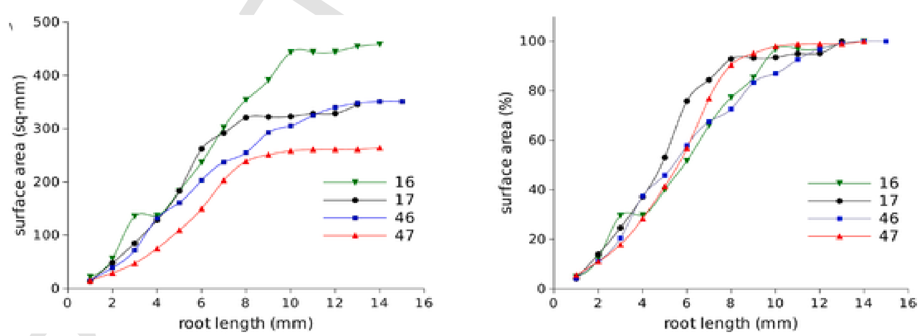

Fig. 10. Relationship of RL and tRSA of two multi-rooted tooth types-maxillary and mandibular first and second molars. The graph on the left shows the net remnant tRSA of the maxillary and mandibular first and second molars. The graph on the right represents the percentage of remnant tRSA for the same tooth types.

reduction range and surging to 49.6 % for RL reductions beyond 8 mm, making it the tooth type with the highest CSA contribution.

For the mandibular central incisor (#41), CSA contributes 9.6 % of tRSA during the first 3 mm of RL reduction and reaches 30.6 % when more than 8 mm of RL reduction occurs. Similarly, the mandibular canine (#43) demonstrates a smaller increase, with CSA rising from 2.3 % within the 1–3 mm reduction range to 31 % for RL reductions greater than 8 mm. Lastly, the mandibular first molar (#46) shows a mild CSA contribution of 1.6 % within the 1–3 mm RL reduction range and climbs to 38.7 % at more than 8 mm RL reduction, reflecting a similar trend to the maxillary first molar, though to a lesser extent. These quantitative observations highlight significant variations in CSA across different tooth types as illustrated in Fig. 12, with molars generally exhibiting higher proportions than incisors and canines. A 9 mm RL reduction at the maxillary first molar (#16) moves the root level above the root trifurcation whereas the same amount of RL reduction at the mandibular first molar keeps the root level apical to the root bifurcation.

4. Discussion

This study used 3D models of human permanent teeth to characterise the geometric relationship between root length (RL) and root surface area (RSA). STL files of teeth were obtained from a commercial source and Meshmixer was used to segment the roots from the crowns at the cemento-enamel junction (CEJ). Root length was measured from the root apex to the CEJ's highest inflection point. To calculate RSA, an algorithm was developed in Python that uses principal component analysis to identify the tooth's long axis and create horizontal slices along the root's long axis in 1 mm increments from the apex. The cir-

Table 9
Average percentage reduction in tRSA with every 1 mm of root length reduction.

Maxillary	#11	#12	#13	#14	#15	#16	#17
Original root length (mm)	17	16	19	17	15	14	13
First 1–3 mm (%)	−1.06	3.03	1.08	1.74	3.15	−0.66	1.32
Next 5 mm (%)	18.85	22.15	14.24	20.90	22.90	21.73	14.63
Beyond 8 mm (%)	26.81	32.51	28.53	34.51	34.85	26.42	20.92
Mandibular	**#41**	**#42**	**#43**	**#44**	**#45**	**#46**	**#47**
Original root length (mm)	12	13	16	14	14	15	14
First 1–3 mm (%)	6.06	3.98	2.04	3.51	−1.53	1.36	−0.50
Next 5 mm (%)	46.84	29.63	21.32	24.61	37.06	19.37	15.54
Beyond 8 mm (%)	14.59	25.36	29.61	36.39	18.29	29.45	21.06

Table 10
Observations of the impact of root length (RL) reduction on the total root surface area (tRSA) from three maxillary teeth (Tables 3–5).

Tooth	Up to 3 mm RL reduction	Between 4 and 8 mm RL reduction	More than 8 mm of RL reduction
#11	A 1 mm reduction (17 mm–16 mm) results in a 5.88 % decrease in RL and only a 0.06 % reduction in tRSA. A 2 mm reduction (17 mm–15 mm) leads to an 11.77 % RL decrease and a 1.43 % tRSA reduction. These findings suggest that minor RL reductions have a negligible impact on tRSA for this tooth.	Reductions in this range show a more pronounced effect. A 4 mm reduction (17 mm–13 mm) leads to a 23.53 % decrease in RL and a 0.25 % reduction in tRSA. A 6 mm reduction (17 mm–11 mm) results in a 35.29 % RL decrease and a more substantial 19.05 % tRSA reduction. This indicates a non-linear relationship between RL reduction and tRSA reduction.	Reductions beyond 8 mm show a considerable impact on tRSA. An 8 mm reduction (17 mm–9 mm) results in a 47.06 % RL decrease and a 36.96 % tRSA reduction. Greater reductions further amplify this trend, indicating that significant RL reductions substantially diminish tRSA for this tooth.
#13	A 1 mm reduction (19 mm–18 mm) results in a 5.26 % RL decrease and a negligible 0.10 % reduction in tRSA. A 2 mm reduction (19 mm–17 mm) leads to a 10.53 % RL decrease and a 1.28 % tRSA reduction. Minor RL reductions show minimal impact on tRSA for this tooth.	A 5 mm reduction (19 mm–14 mm) leads to a 26.32 % RL decrease and a 5.05 % tRSA reduction. An 8 mm reduction (19 mm–11 mm) results in a 42.11 % RL decrease and a 31.51 % tRSA reduction.	Reductions beyond 8 mm show a significant impact. A 10 mm reduction (19 mm–9 mm) results in a 52.63 % RL decrease and a 48.14 % tRSA reduction. Larger reductions further amplify this trend, highlighting the substantial impact on tRSA from significant RL reductions.
#16	A 1 mm reduction (14 mm–13 mm) leads to a 7.14 % decrease in RL and a negligible 0.06 % reduction in tRSA. A 2 mm reduction (14 mm–12 mm) shows a 14.29 % RL decrease and a 0.20 % tRSA reduction. Minor RL reductions have a minimal impact on tRSA.	A 4 mm reduction (14 mm–10 mm) leads to a 28.57 % RL decrease and a −2.24 % tRSA reduction. Notably, the tRSA increases slightly, suggesting that the initial 4 mm reduction might remove a portion of the root with a higher surface area concentration. A 6 mm reduction (14 mm–8 mm) results in a 42.86 % RL decrease and a 20.28 % tRSA reduction.	An 8 mm reduction (14 mm–6 mm) shows a substantial impact, resulting in a 57.14 % RL decrease and a 46.72 % tRSA reduction. Larger reductions further amplify this trend, emphasizing the significant impact on tRSA from more substantial RL reductions.

cumferential root surface area (cRSA), cross-sectional area (CSA), and total root surface area (tRSA) were then determined. The study found that tRSA decreases with root length reduction, with the steepest reductions occurring beyond 50 %. The contribution of CSA to tRSA increases with greater RL reduction, particularly when reduction exceeds 8 mm.

Table 11
Observations of the impact of root length (RL) reduction on the total root surface area (tRSA) from three mandibular teeth (Tables 6–8).

Tooth	Up to 3 mm RL reduction	Between 4 and 8 mm RL reduction	More than 8 mm of RL reduction
#41	A 1 mm reduction (12 mm–11 mm) leads to an 8.33 % decrease in RL and a −2.23 % reduction in tRSA. A 2 mm reduction (12 mm–10 mm) results in a 16.67 % RL decrease and a 5.10 % tRSA reduction. Notably, the tRSA increases with the initial 1 mm reduction, similar to observations in maxillary molars.	A 4 mm reduction (12 mm–8 mm) results in a 33.33 % RL decrease and a 25.88 % tRSA reduction. A 6 mm reduction (12 mm–6 mm) leads to a 50.00 % RL decrease and a more pronounced 47.25 % tRSA reduction.	An 8 mm reduction (12 mm–4 mm) leads to a 66.67 % RL decrease and a 67.05 % tRSA reduction. Larger reductions further amplify this trend, with tRSA reduction slightly greater than RL reduction.
#43	A 1 mm reduction (16 mm–15 mm) shows a 6.25 % RL decrease and a negligible 0.02 % tRSA reduction. A 2 mm reduction (16 mm–14 mm) leads to a 12.5 % RL decrease and a 1.52 % tRSA reduction. Minor RL reductions have a minimal impact on tRSA for this tooth.	A 4 mm reduction (16 mm–12 mm) results in a 25 % RL decrease and a 9.04 % tRSA reduction. A 7 mm reduction (16 mm–9 mm) results in a 43.75 % RL decrease and a 27.53 % tRSA reduction.	An 8 mm reduction (16 mm–8 mm) leads to a 50.00 % RL decrease and a 34.82 % tRSA reduction. Larger reductions further amplify this trend, indicating a substantial impact on tRSA with significant RL reductions.
#46	A 1 mm reduction (15 mm–14 mm) leads to a 6.67 % decrease in RL and a negligible 0.00 % reduction in tRSA. A 2 mm reduction (15 mm–13 mm) results in a 13.33 % RL decrease and a 0.90 % tRSA reduction. Minor RL reductions have a minimal impact on tRSA for this tooth.	A 4 mm reduction (15 mm–11 mm) results in a 26.67 % RL decrease and a 7.40 % tRSA reduction. A 6 mm reduction (15 mm–9 mm) leads to a 40.00 % RL decrease and a 16.64 % tRSA reduction.	An 8 mm reduction (15 mm–7 mm) shows a substantial impact, resulting in a 53.33 % RL decrease and a 32.46 % tRSA reduction. Larger reductions further amplify this trend, highlighting the considerable impact on tRSA with significant RL reductions.

4.1. Assessment of methodology

The study's methodology explained how the Python algorithm, combined with anatomically representative 3D surface mesh models, enabled the precise and direct measurement of the cRSA and CSA at both full root length and at various simulated root lengths. This simulation was achieved by virtually “shortening" the root in the 3D tooth model in 1 mm increments that was adapted from a previous study [10]. It allowed the present study to assess the impact of root shortening in a systematic manner on RSA.

The significant and unique value of the present study is the determination of CSA at each simulated level of root reduction which was not carried out in previous three-dimensional computer-aided studies on the RSA [6–11]. The CSA, together with the cRSA, makes up the remnant attachment to the alveolar bone. Excluding CSA from tRSA calculations in previous studies significantly limits understanding of how root length shortening impacts tooth longevity. This omission risks misinterpreting the true effects of substantial root length shortening on a tooth's function and long-term viability.

The high-resolution 3D teeth models used in the study are anatomically realistic and representative of the tooth's morphology - the crown, root, and cementoenamel junction. What is known about the set of 3D teeth models is the gender, age group and ethnicity from which the models were derived. Compared with previous studies that determined RSA from extracted human teeth [6–9,11], the use of this set of 3D teeth models eliminated anatomic variations of root morphology associated

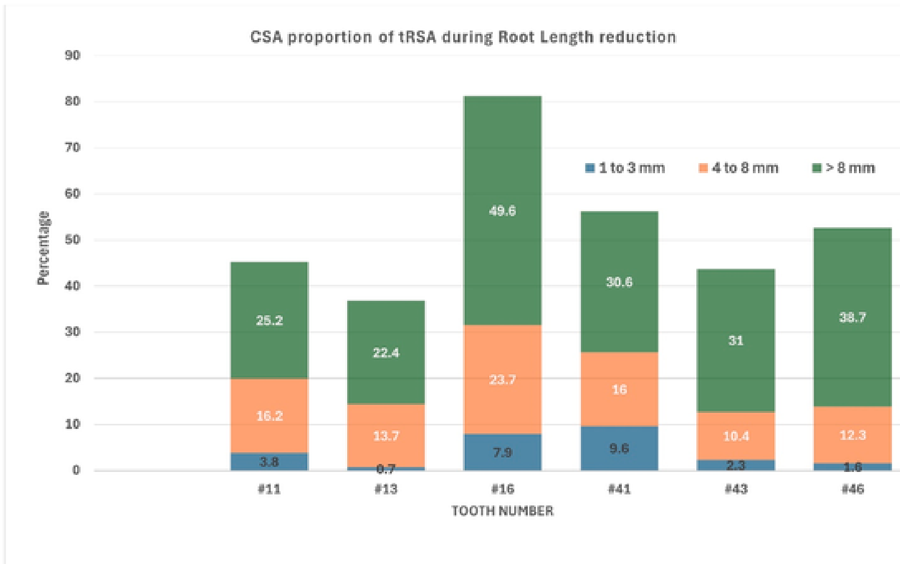

Fig. 11. The average percentage of CSA to tRSA in the three intervals of RL reduction.

with actual teeth and permitted the study to establish a baseline geometric relationship between RSA and root length.

Two studies involving direct manual measurements on extracted teeth established baseline data on root length, root diameter, and taper for single-rooted adult European teeth [4,5]. Another study [14] highlighted the advantages of automated measurements over manual methods for assessing tooth dimensions. Additional studies [9,11] demonstrated the effectiveness of computer-aided 3D techniques for measuring the RSA of extracted human teeth. While these computer-aided methods improve accuracy, repeatability, and reproducibility, they require specialised equipment, software, and expertise to acquire and process 3D images. These advancements supported the rationale for adopting Python programming in the present study to develop an accessible and accurate method for measuring root length and RSA.

The identification and segmentation of the root at the digital CEJ is a potential source of error that may affect the accuracy of RL and RSA measurements. The study of European anterior teeth [4] suggested that variations in root length and taper measurements could result from the “sinuosity” or curvilinear nature of the CEJ. In the present study, the CEJ was identified for all 14 tooth types by a single experienced clinician in one session. This approach introduces the possibility of inconsistency in defining the CEJ, as it is not clearly demarcated on the surface of the 3D tooth models, potentially affecting RL and RSA measurements.

An important aspect not accounted for by the algorithm was the concept of “Partial Volume Changes. Localised loss of tooth structure at the root surface, without significant changes in overall root length, can occur in cases of EARR. In this study, the focus was placed on establishing a general geometric relationship between RL and tRSA. While EARR remains an important consideration, it was not the primary focus of the investigation. It is acknowledged that the methodology might not capture subtle, localised changes in root surface area caused by EARR if those changes do not significantly alter overall root length.

4.2. Total root surface area

Excluding third molars, the tRSA for all 14 teeth was 3549.88 mm^2. Incisors and canines contributed 34.71 % (1232.17 mm^2), premolars 26 % (922.98 mm^2), and molars 39 % (1384.52 mm^2). This tRSA closely aligns with the mean RSA (3613.9 mm^2) reported for a Chinese population [9] but is lower than the RSA (3869.7 mm^2) recorded for a Japanese population [7]. These findings indicate that the 3D anatomical models used in this study are comparable to and representative of permanent teeth from human populations. The higher RSA observed in the Japanese study may be attributed to its use of a membrane coating method as a proxy for root surface area, which likely accounted for morphological factors such as root curvature.

4.3. Root length

As shown in Table 12, the root lengths of the 3D tooth model for #11, #12, #14, and #45 exceed one standard deviation above the mean root lengths reported in previous studies [4,5,7,9]. This difference may be due either to study-specific sample anatomical variations or differences in the methods used to measure RL. In contrast, the RL measurements for the other 10 tooth types fall within one standard deviation of the mean RL reported in these studies.

4.4. Root surface area

A comparison of tRSA values from the present study (Table 13) with previous studies [7,9,11] reveals no clear correlation between RL and RSA. For example, while the RL of #13 in the present study is 19 mm, longer than the RL reported for the same tooth in two previous studies [7,9], its corresponding tRSA is the lowest among the three. This discrepancy could be attributed to variations in root diameter and morphology, particularly in the middle or cervical segments of the root. These findings highlight an important clinical insight: for maxillary canines, root length alone is insufficient to estimate root surface area or the corresponding periodontal attachment area.

The maxillary first molar (444.17 mm^2) and the mandibular first molar (351.01 mm^2) exhibited the largest tRSAs in their respective arches, with values within one standard deviation of the RSA measurements reported by a previous 3D study on extracted human teeth [9]. The maxillary and mandibular second molars have the next highest tRSA at 328.67 mm^2 and 260.67 mm^2, respectively. That first and second molars have the largest and second largest root surface areas also support the common orthodontic practice of using them as mechanical anchors during the retraction movements of the upper and lower front teeth which have smaller root surface areas. Where the pressure applied to the periodontal ligament surrounding the root surface is calculated by the force applied to the tooth crown divided by the tooth's RSA, the

Fig. 12. Variation in cross-sectional shape and size at specific simulated RL reduction levels.

resultant pressure on front teeth with smaller RSAs is therefore higher than those at the first and second molars, resulting in movements of the front teeth while the molars stay anchored within the jawbone.

Consistent with the findings from a previous study on RSA in canines and premolars [8], this study found that the mandibular canine has a larger tRSA than either mandibular premolar, while the first and second premolars exhibit similar tRSAs. The larger tRSA of the mandibular canine can be attributed to its longer root compared to the single-rooted mandibular premolars, which has implications for orthodontic mechanics. Orthodontic movement of the mandibular canine requires sufficient anchorage, either from the first molar/premolar region or the adjacent front teeth, to counteract applied forces.

Among the maxillary teeth, the lateral incisors demonstrated the smallest tRSA (206.19 mm^2), consistent with findings from a previous CBCT analysis [11]. This result is unsurprising, as the root of the maxillary lateral incisor (#12) has the narrowest mesio-distal width of the 7 maxillary tooth types. Clinically, this information is significant because, under equal force applied from the first molars to the four maxillary incisors, the lateral incisors experience the highest pressure due to their smaller RSA. This increased pressure heightens the risk of EARR. Therefore, clinicians should exercise caution to minimise the risk of EARR in maxillary lateral incisors during retraction movements of the maxillary teeth.

Table 12
Comparisons of root lengths for each tooth type (excluding 3rd molars) (mm).

Tooth type	This study	Yamamoto et al.	Gu et al.	Fantozzi et al.[a]	Bernadi et al.[b]
Maxillary central incisor	17	12.2	14.16	13.5	–
Maxillary lateral incisor	16	13.4	14.20	13.6	–
Maxillary canine	19	16.6	17.61	16.5	–
Maxillary 1st premolar	17	12.9	13.2	–	13.5
Maxillary 2nd premolar	15	13.9	13.31	–	14.9
Maxillary 1st molar	14	13.5	12.28	–	–
Maxillary 2nd molar	13	12.7	12.44	–	–
Mandibular central incisor	12	12.0	12.05	13.5	–
Mandibular lateral incisor	13	12.6	13.18	13.5	–
Mandibular canine	16	14.9	16.51	15.8	–
Mandibular 1st premolar	14	14.7	14.03	–	14.4
Mandibular 2nd premolar	14	14.0	13.88	–	15.4
Mandibular 1st molar	15	12.6	13.16	–	–
Mandibular 2nd molar	14	12.6	13.16		–

[a] Study confined to anterior teeth – central incisors, lateral incisors and canines.
[b] Study confined to premolars – first and second premolars.

Table 13
Comparisons of mean root surface area for each tooth type (excluding 3rd molars) (mm^2).

Tooth type	This study	Yamamoto et al.	Gu et al.	Lakhani et al.
Maxillary central incisor	239.47	200.7	195.24	213.2
Maxillary lateral incisor	206.19	202.9	181.54	175.1
Maxillary canine	265.42	291.9	275.54	322.1
Maxillary 1st premolar	291.90	249.4	229.77	286.5
Maxillary 2nd premolar	239.01	232.9	221.41	231.04
Maxillary 1st molar	444.17	467.7	410.45	375.45
Maxillary 2nd molar	328.67	368.4	383.02	351.05
Mandibular central incisor	143.80	159.5	140.38	209.3
Mandibular lateral incisor	158.49	180.0	164.96	231.4
Mandibular canine	218.80	265.2	255.71	230.7
Mandibular 1st premolar	197.90	237.5	195.78	194.3
Mandibular 2nd premolar	194.17	212.4	195.95	227.08
Mandibular 1st molar	351.01	432.8	391.60	391.76
Mandibular 2nd molar	260.67	368.4	372.75	359.97

4.5. Geometric relationship between RL and RSA

4.5.1. (a) Root length reduction of up to 3 mm

For the first 3 mm of simulated root shortening, five out of seven maxillary tooth types showed minimal RSA reduction (under 5 % on average). Similarly, five out of seven mandibular tooth types exhibited less than 7 % RSA reduction. This observation of minimal RSA reduction, common to both maxillary and mandibular teeth, can be explained by the narrow conical morphology characteristic of the apical root segment. Accordingly, we infer that the loss of linear root length for the first 3 mm has little impact on the overall periodontal surface area attachment of the root. A European study [4] described root tapering as a percentage of change in diameter between three points on the root at the coronal third (2 mm below the CEJ, the middle third (4 mm from CEJ), and apical third (3 mm from the apex). It noted that tapering generally becomes more pronounced as you move from the CEJ toward the apex, indicating that the diameter of the root decreases more rapidly in the apical third of the root compared to the coronal third. Our study's use of the 3 mm root length threshold from the root apex aligns with the apical threshold mark [4] and acknowledges that the increased taper of the root at the apical third is consistent with the minimal reduction in RSA from root length reduction of up to 3 mm.

Interestingly, two maxillary teeth (#11 and #16) and two mandibular (#45 and #47) teeth exhibited a gain in average RSA, likely due to their broad cross-sectional root areas. For the maxillary central incisor and first molar, the broad cross-sectional areas calculated at the 3rd mm mark of simulated shortening likely contributed to the increased remnant RSA (Tables 3 and 5). Similarly, the broad cross-sectional root areas at the 1st/2nd mm and 2nd mm of simulated root reduction for the mandibular second premolar and second molar, respectively, may have led to the marginal gain in RSA.

4.5.2. (b) Between 4 and 8 mm of root length reduction

Beyond the first 3 mm of simulated root length shortening, the tRSA reduction was substantial compared to the initial 3 mm. This observation corresponds to the anatomic construct of the tooth root, where the more cervical segments exhibit a more parallel-sided, cylinder-like shape in contrast to the conical shape of the apical segment.

The average tRSA reduction from the 4th to 8th mm of root length reduction was less pronounced in maxillary teeth. No maxillary teeth exceeded 25 % of tRSA reduction, whereas only four mandibular tooth types showed less than 25 % of tRSA reduction. The mandibular teeth with greater than 25 % of RSA reduction - the central and lateral incisors and the second premolar - are teeth with a smaller root circumference at the middle root segment.

The proportion of periodontal attachment area lost per millimeter of vertical root resorption becomes less favorable beyond the first 3 mm of apical root reduction. The findings from a previous study [10] confirm this trend which show a substantial increase in the average percentage reduction in tRSA after the initial 3 mm of apical root shortening. This observation holds significant clinical relevance: the impact of severe external apical root resorption (EARR) (≥4 mm) varies among teeth depending on their root circumference and morphology. Teeth with longer roots and broader circumferences, such as molars and canines, retain a larger tRSA for a given amount of EARR compared to teeth with shorter, slender roots, like lateral and central incisors. Single-rooted incisors with ≥4 mm of EARR will have a smaller remaining periodontal attachment area than multi-rooted teeth with the same degree of resorption. Clinicians managing EARR in incisors must emphasise the importance of excellent oral hygiene to patients, as any loss of crestal bone height from periodontal disease could further reduce the already compromised periodontal attachment area. Additionally, the biomechanics of orthodontic movements for such incisors must be adjusted to account for changes in the tooth's center of resistance caused by root shortening.

Root surface area is influenced not only by root length but also by factors such as the number of roots, their curvature, and furcations, as observed in molars, which collectively contribute to tRSA [11]. These anatomical features enable teeth with significant EARR to retain sufficient periodontal attachment area, allowing them to function normally and remain stable within the oral environment.

4.5.3(c). Root length reduction beyond 8 mm

The highest tRSA reductions of three levels of RL shortening are seen for all seven maxillary tooth types when RL reduction exceeds 8 mm. The reductions are most significant in this segment, ranging from 20.92 % (#17) to 34.85 % (#15). Teeth #14 and #15 show the greatest tRSA reduction at 34.41 % and 34.85 %, respectively, likely due to the tapering geometry of their roots, which causes a sharper decline in RSA as more root length is lost. Mandibular teeth show substantial reductions in tRSA, ranging from 14.59 % (#41) to 36.39 % (#44). The latter's conical root morphology may accelerate tRSA loss with greater RL reductions. The interpretation of RL reductions beyond 8 mm, i.e., from the 9th millimeter of root length, has to be based on the remaining root length of the tooth type. At the 9th millimeter of root length, only three teeth - #11, #13 and #14 – have ≥50 % of its RL intact. The RL of the remaining 11 teeth, at the 9th mm of remaining root length, have less than 50 % of RL. The mandibular central and lateral incisors are most at risk of poor tooth longevity and increased tooth mobility due to their much shorter root length, smaller girth and tRSA when RL reductions exceed 8 mm even though their average tRSA reduction is lower when compared with longer single-rooted teeth and multi-rooted teeth. All four molar tooth types, even with more than 8 mm of RL reduction and less than 50 % of their original RL remaining, demonstrate broader girths and relatively higher CSA. These attributes suggest that such significant RL reduction poses a lower risk to tooth longevity compared to mandibular incisors.

4.6. Contribution of CSA to tRSA

The contribution of CSA to tRSA increases progressively with RL reduction, becoming particularly significant beyond 8 mm. This trend reflects the growing importance of CSA as the cRSA diminishes with progressive root shortening. Molars, with their broader root girth and multiple roots, exhibit the highest CSA proportions during RL reductions exceeding 8 mm. In contrast, single-rooted incisors and canines, characterised by narrower and more tapered roots, contribute smaller CSA proportions under similar conditions.

Teeth with higher CSA proportions, such as molars, are better equipped to retain periodontal support despite substantial RL loss. The apical 1–3 mm of the root, being conical and narrower, accounts for a minimal CSA contribution compared to RL reductions of 4 mm or more. As RL reductions reach 4–8 mm, the gradual increase in root girth and circumference leads to a modest rise in CSA's contribution to tRSA. This reflects a transition from the narrower apical root segment to the broader cervical portion of the root.

Clinically, teeth experiencing RL reductions of 4–8 mm can retain sufficient periodontal attachment area, provided crestal bone loss is absent. This highlights the importance of preserving periodontal health, as adequate attachment area at this stage is critical for maintaining tooth stability and function.

4.7. Possibility of applying algorithm to CBCT teeth images

The potential clinical value of integrating the study's algorithmic analysis of RSA into a CBCT-based orthodontic treatment planning protocol is worth exploring. Having the ability to predict the biomechanical behavior of teeth with varying root lengths and RSAs could significantly enhance treatment planning, allowing clinicians to (i) anticipate potential challenges and limitations associated with reduced root surface area, (ii) optimize force systems applied to teeth to achieve predictable and safe tooth movement, and (iii) minimise the risk of complications like root resorption. The principles underlying the study's algorithm, calculating cRSA and CSA along the root could theoretically be adapted for CBCT data. However, directly applying the algorithm to CBCT scans presents several challenges: (i) CBCT images generally have lower resolution than the 3D models used in the study, which could affect the accuracy of tooth segmentation and RSA calculations, (ii) CBCT images are prone to noise and artefacts, which can further complicate segmentation and measurement accuracy, and (iii) the algorithm would need to be modified and validated for CBCT data, accounting for the specific characteristics and limitations of this imaging modality.

Despite the challenges, a conceptual protocol with steps involved in integrating the study's algorithmic analysis into CBCT-based treatment planning are: (i) obtain a high-resolution CBCT scan of the patient, (ii) develop or adapt segmentation algorithms specifically for CBCT data to accurately isolate the teeth of interest, (iii) apply modified versions of the study's algorithm to calculate RL and tRSA from the segmented teeth, and (iv) integrate the root length and tRSA data into biomechanical simulation software to predict tooth movement under different force. To be able to do the above, there is a need for further research to develop and validate biomechanical models that incorporate RL and RSA data to predict tooth movement accurately. An interdisciplinary collaboration between dentists, computer scientists, and engineers is needed to achieve the goal of integrating this analysis into clinical practice.

4.8. Anatomical complexity influencing the RL-RSA relationship

Apart from the distinction between single-rooted and multi-rooted teeth, several anatomical and pathological factors may significantly influence RSA changes during root length reduction by adding complexity into the RL-RSA relationship beyond root number alone. Although these factors were not explicitly accounted for in this study, they warrant further consideration when evaluating the RL-RSA relationship.

First, variations in root curvature, ranging from straight to complex curves (including root dilacerations), may create non-linear relationships between root length reduction and surface area changes. Curved roots tend to have a larger surface area due to their increased length along the curve. As a result, more pronounced root curvatures may cause greater tRSA loss up to 8 mm of root shortening compared to straight roots. This reduction in surface area could also affect periodontal support during orthodontic tooth movement.

Second, periodontal bone loss, including horizontal and angular patterns, can reduce the root surface area available for periodontal ligament attachment. As bone loss progresses, the functional root surface area (RSA) decreases. Significant crestal bone loss exposes more of the root, reducing RSA and increasing the risk of tooth mobility. If apical root shortening occurs alongside crestal bone loss, the decline in RSA accelerates.

Third, in multi-rooted teeth, variations in root furcation levels may influence how RSA distributes along the root length. Teeth with longer root trunks, where the furcation is further away from the cemento-enamel junction (CEJ), retain more RSA during RL reduction because their larger unbranched portion provides substantial CSA and cRSA at and above the furcation level. In contrast, teeth with shorter root trunks, where the furcation is closer to the CEJ, lose a greater proportion of total root surface area (tRSA) for the same amount of root length (RL) reduction. This occurs because their roots divide earlier, so a significant portion of RSA is lost more quickly as RL decreases.

Fourth, irregular cross-sectional root morphologies [15], such as C-shaped, kidney, and hourglass shapes, as well as concavities [16], can alter the mathematical relationship between root length and surface area. These morphologies often reduce the cross-sectional area (CSA) at certain points along the root compared to those with a more globular or rounder cross-section, while simultaneously increasing the root's circumferential length. This increase in circumference leads to a greater circumferential root surface area (cRSA), thereby contributing more substantially to the total root surface area (tRSA). As a result, when root length is reduced - whether through resorption, surgical shortening, or other processes - roots with these irregular features may experience a greater proportional decrease in tRSA than those with more uniform cross-sections. This occurs because their increased cRSA amplifies the surface area lost per unit of root length removed. Clinically, this may influence factors such as periodontal attachment, anchorage, or the biomechanical behavior of the root under functional loads.

4.9. Limitations of using commercial digital tooth models

This study relied on a single set of commercial digital tooth models to analyze the geometric relationship between RL and RSA. While these models offer a standardized and reproducible dataset for geometric analysis, they do not reflect the natural variability seen in clinical teeth. Real tooth roots vary significantly in shape and size, whereas the selected commercial models likely represent a narrow subset of this diversity. This limitation reduces the generalizability of the findings. Additionally, anatomical complexities discussed in the previous section, as well as conditions such as external apical root resorption (EARR), may significantly affect the RL-RSA relationship in actual patients. Variations in root morphology across different ethnicities, age groups, and clinical conditions further contribute to anatomical complexity, which is not captured in our dataset. Consequently, the study's findings may not fully translate to clinical cases where these factors are present.

4.10. Future research directions

To comprehensively understand the relationship between root length and root surface area in clinical scenarios, we propose six interconnected areas of research that address both anatomical complexities and the limitations of the current commercial models.

This research series begins with a critical validation study that examines geometric relationships across different malocclusion categories. Investigators will compare commercial tooth models with pre-treatment CBCT-segmented teeth from Class I, Class II Division 1, Class II Division 2, and Class III adult patients with no history of orthodontic treatment or tooth trauma. This comparison will determine whether standardized models accurately represent real-world RL-RSA relationships. The findings will establish essential baseline data and a methodological framework for future studies.

Building on this validation, the second research direction adopts a multi-center approach using pre-treatment CBCT data to examine population- and age-related variations. By analyzing ethnic differences across at least three populations and age groups (20–35, 36–50, and 51–65 years), investigators will determine whether RL-RSA geometric relationships require population- and age-specific adjustments. This study will refine models to better reflect population- and age-specific variations in clinical practice.

The third research direction investigates how external apical root resorption (EARR) affects RL-RSA relationships. Using matched pairs of segmented CBCT images taken before and after orthodontic treatment, researchers will quantify how different resorption patterns influence RSA changes. This study has two key components. First, it examines apical root resorption, where length reduction primarily occurs at the apex. Second, it analyzes partial volume changes along the root surface, where overall root length remains relatively unchanged, but localised resorption causes surface irregularities and cavitations. This dual approach will help clinicians distinguish between length-dependent RSA loss and surface erosion, particularly in cases where root shortening may not be apparent. The study will also compare how these resorption patterns influence the RL-RSA relationship in single-rooted versus multi-rooted teeth. These findings will improve risk assessment and treatment modifications in orthodontic cases, especially in cases where conventional root length measurements may underestimate RSA loss.

The fourth research direction examines how root curvature and root surface contour affect RSA following RL reduction. Investigators will use detailed CBCT analysis to evaluate variations in root structure, ranging from straight to complex curves, along with irregular morphologies and concavities. This study will determine how different degrees of curvature influence RSA loss and whether specific contour features predispose roots to greater proportional reductions in surface area. Understanding these variations will enhance clinical decision-making, particularly in cases requiring orthodontic movement.

The fifth research direction focuses on multi-rooted teeth, specifically how furcation levels influence surface area calculations and distribution. Pre-treatment CBCT data will be analysed alongside micro-CT imaging of extracted multi-rooted teeth with varying furcation levels. Since CBCT data may not possess the full extent of furcation variation, extracted teeth will help expand the sample, providing a more comprehensive understanding of RL-RSA relationships in multi-rooted dentition. This study will clarify how anatomical furcation differences impact RSA loss during root shortening.

The sixth research direction extends the fifth by examining how periodontal bone loss affects RL-RSA relationships. Using CBCT imaging and clinical attachment loss measurements, investigators will conduct paired comparisons of multi-rooted teeth with and without bone loss. This method will isolate the effects of crestal bone loss while controlling for individual variability in root shape, size, and anatomy. The study will assess how different severities and patterns of bone loss influence RSA loss and whether specific thresholds exist for clinical decision-making. These findings will provide essential insights for predicting tooth stability, refining periodontal treatment strategies, and optimizing orthodontic interventions in patients with compromised periodontal support or EARR.

Together, these six research directions offer a comprehensive framework for understanding how clinical, anatomical, ethnic, and age-related factors influence the geometric relationship between root length and surface area. Addressing these key variables will improve precision in treatment planning and risk assessment, particularly in cases where root length reduction is a concern. Additionally, the findings will help establish RSA thresholds for clinical decision-making, which in turn strengthens the practical application of RL-RSA analysis in evidence-based dental practice.

4.11. Clinical significance and implications of findings

This study used a Python algorithm to simulate root length loss through sequential plane cuts at 1 mm intervals from the root tip. The virtual removal of the entire apical section of the root represents a “worst-case" scenario of EARR. Such a scenario is rare in clinical practice, and the findings should be interpreted with this context in mind.

The geometric relationship between RL and tRSA revealed by this study offers several clinically significant insights to guide treatment decisions, particularly in managing EARR cases. The findings highlight that the contribution of CSA to tRSA becomes increasingly significant as RL reductions exceed 3 mm. Clinicians should take note of this important feature when evaluating the impact of RL loss, as CSA can play a crucial role in maintaining periodontal attachment and tooth stability in advanced cases of EARR.

Teeth with EARR up to 3 mm generally experience minimal reductions in tRSA, typically less than 7 %. This is attributed to the narrow, conical shape of the apical root segment, which contributes less to the overall root surface area. As a result, these teeth are likely to retain sufficient periodontal support for long-term stability. Treatment in such cases should prioritise identifying and addressing the underlying cause of resorption, whether related to orthodontic forces, trauma, or other factors. Regular monitoring is essential to detect progression and guide appropriate management.

However, when EARR exceeds 3 mm ($\geq$4 mm), the reduction in tRSA becomes significantly more pronounced. Beyond the initial 3 mm of root shortening, further loss occurs predominantly in the broader middle and cervical regions of the root, where each additional millimeter of resorption leads to a greater loss of surface area. This substantial reduction in RSA can compromise tooth stability and requires careful evaluation during treatment planning. Tooth-specific characteristics, such as root morphology and type, must also be considered for risk management of the affected teeth when RL loss is 4 mm or more. Multi-rooted teeth and those with longer single and broader roots tend to retain more tRSA for a given amount of EARR compared to teeth with shorter, slender roots.

Accurately measuring RSA that includes CSA, provides a more precise representation of the remaining periodontal support following EARR. This accurate assessment is critical for predicting tooth longevity and tailoring treatment decisions to the specific needs of each case. Clinicians are encouraged to adopt assessment techniques such as small field-of-view high spatial resolution CBCT imaging (≤0.2 mm) that can precisely account for the three-dimensional nature of root morphology and its impact on periodontal attachment. Treatment planning for teeth affected by EARR should factor in the relationship between root length, root girth, RSA, and the potential for future resorption. For orthodontic cases, special biomechanical considerations must be made, as the tooth's center of resistance shifts with reduced root length, potentially altering force application and movement patterns.

The findings of this study emphasise the importance of evaluating CSA and tRSA alongside root length when assessing the impact of EARR on tooth prognosis. By utilising 3D assessment methods and integrating these insights into clinical decision-making, clinicians can improve patient care and better manage the long-term stability of teeth affected by EARR.

5. Conclusion

This study provides valuable insights into the geometric relationship between root length (RL) and root surface area (RSA) using standardized digital tooth models. By defining a baseline RL-RSA relationship in Japanese male adults, our findings serve as a useful reference for clinicians and researchers. Although commercial models offer a controlled and standardized environment, their limitations warrant cautious interpretation. Real clinical teeth exhibit significant anatomical variability, including differences in root curvature, periodontal bone loss, furcation levels, and irregular morphology. Since these complexities were not fully captured in our dataset, further research is needed to validate our findings using real clinical teeth. Future studies should incorporate high-resolution three-dimensional imaging and computational modelling to analyze root geometry and morphology in diverse populations. In particular, validation using pre-treatment CBCT scans from a broader range of adult orthodontic patients would enhance the clinical applicability of our findings. Such validation would provide a more clinically relevant foundation for understanding the RL-RSA relationship. Establishing a more comprehensive understanding of the RL-RSA relationship in real-world contexts will support precise treatment planning, improve risk assessment, and optimize clinical outcomes in procedures where root length reduction is a concern.

CRediT authorship contribution statement

Chloe Xiao Wei Chan: Writing – review & editing, Writing – original draft, Data curation, Conceptualization. **Wee Kheng Leow:** Supervision, Software, Methodology. **Alan Ho-lun Cheng:** Supervision, Software, Methodology. **Kelvin Weng Chiong Foong:** Writing – review & editing, Supervision, Project administration, Conceptualization.

Ethics statement

The study titled "The geometric relationship between root length and root surface area determined from digital tooth models" was a purely computer-based study and did not involve any human subjects, animal subjects, or direct interaction with personal data. The 3D anatomic tooth models were purchased from a commercial online vendor. Ethical approval was deemed unnecessary as the research solely utilized these models.

The research was conducted with transparency, integrity, and a commitment to maintaining the highest standards of academic and scientific rigor. The authors declare no conflicts of interest and affirm that no external influences compromised the outcomes of this study.

Funding

This research did not receive any specific grant from funding agencies in the public, commercial, or not-for-profit sectors.

Declaration of competing interest

The authors declare that they have no known competing financial interests or personal relationships that could have appeared to influence the work reported in this paper.

Appendix A. Supplementary data

Supplementary data to this article can be found online at https://doi.org/10.1016/j.compbiomed.2025.110189.

References

[1] N. Brezniak, A. Wasserstein, Orthodontically induced inflammatory root resorption. Part I- the basic science aspects, Angle Orthod. 72 (2) (2002) 175–179.
[2] D.N. Remington, et al., Long-term evaluation of root resorption occurring during orthodontic treatment, Am. J. Orthod. Dentofacial Orthop. 96 (1) (1989) 43–46.
[3] W.S. Parker, Root resorption- long-term outcome, Am. J. Orthod. Dentofacial Orthop. 112 (2) (1997) 119–123.
[4] G. Fantozzi, et al., Analysis of the root morphology of European anterior teeth, Ital. J. Anat Embryol. 118 (1) (2013) 78–91.
[5] S. Bernardi, et al., Morphometric study on single-root premolars in a European population sample: an update on lengths and diameters, Eur. J. Anat. 23 (1) (2019) 17–25.
[6] R.M. Dunlap, M.E. Gher, Root surface measurements of the mandibular first molar, J. Periodontol. 56 (4) (1985) 234–238.
[7] T. Yamamoto, et al., Estimation of the remaining periodontal ligament from attachment-level measurements, J. Clin. Periodontol. 33 (3) (2006) 221–225.
[8] J.K. Mowry, et al., Root surface area of the mandibular cuspid and bicuspids, J. Periodontol. 73 (10) (2002) 1095–1100.
[9] Y. Gu, et al., Measurement of root surface area of permanent teeth in a Chinese population, Arch. Oral Biol. 81 (2017) 26–30.
[10] K.L. Kalkwarf, R.F. Krejci, Y.C. P, Effect of apical root resorption on periodontal support, J. Prosthet. Dent 56 (3) (1986) 317–318.
[11] K. Lakhani, V. Vashishth, N. Gugnani, Root surface area measurement of permanent dentition in Indian population – CBCT analysis, Inform. Med. Unlocked 9 (2017) 1–5.
[12] A.D. Mirabella, J. Artun, Prevalence and severity of apical root resorption of maxillary anterior teeth in adult orthodontic patients, Eur. J. Orthod. 17 (1995) 93–99.
[13] L. Linge, B.O. Linge, Patient characteristics and treatment variables associated with apical root resorption during orthodontic treatment, Am. J. Orthod. Dentofacial Orthop. 99 (1) (1991) 35–43.
[14] L. Di Angelo, et al., A new computational method for automatic dental measurement: the case of maxillary central incisor, Comput. Biol. Med. 70 (2016) 202–209.
[15] J. Gellis, R. Foley, A novel system for classifying tooth root phenotypes, PLoS One 16 (11) (2021) e0251953.
[16] K.O. Ghishan, et al., The root complex in posterior teeth: a direct digital analysis, Int. J. Periodontics Restor. Dent. 44 (1) (2024) 27–37.